Atmos. Chem. Phys. Discuss., https://doi.org/10.5194/acp-2017-433
Manuscript under review for journal Atmos. Chem. Phys.
Discussion started: 15 June 2017

Atmospheric Chemistry and Physics Discussions

Influence of NO_2 on secondary organic aerosol formation from ozonolysis of limonene

Changjin Hu[1,§], Qiao Ma[1,2,§], Zhi Liu[1], Yue Cheng[1], Liqing Hao[3], Nana Wei[1], Yanbo Gai[1], Xiaoxiao Lin[1], Xuejun Gu[1], Weixiong Zhao[1], Mingqiang Huang[1,4], Zhenya Wang[1], Weijun Zhang[1,2,5]

[1]Laboratory of Atmospheric Physico-Chemistry, Anhui Institute of Optics and Fine Mechanics, Chinese Academy of Sciences, Hefei 230031, Anhui, China
[2]University of Science and Technology of China, Hefei 230026, Anhui, China
[3]Department of Applied Physics, University of Eastern Finland, Kuopio 70211, Finland
[4]College of Chemistry & Environment, Minnan Normal University, Zhangzhou 363000, P. R. China
[5]School of Environmental Science and Optoelectronic Technology, University of Science and Technology of China, Hefei 230026, Anhui, China

§These authors contributed equally to this work.

Correspondence to: Weijun Zhang (wjzhang@aiofm.ac.cn)

Atmos. Chem. Phys. Discuss., https://doi.org/10.5194/acp-2017-433
Manuscript under review for journal Atmos. Chem. Phys.
Discussion started: 15 June 2017

Atmospheric Chemistry and Physics Discussions

Abstract

Limonene has a strong tendency to undergo ozonolysis to form semi-volatile and low-volatility compounds that contribute to secondary organic aerosols (SOAs) both outdoors and indoors. The influence of NO_2 on SOA formation from ozonolysis of limonene has been evaluated using chamber experiments and the Master Chemical Mechanism (MCM) coupled with a gas-particle partitioning model in this work. A series of 21 indoor chamber experiments were carried out with or without NO_2 under different $[O_3]_0/[VOC]_0$ ratios, and these experimental data were compared with the model simulations. Agreement in SOA yields was observed between the experimental observations and model simulations under varying conditions. Generally, SOA mass yields are positively dependent on $[O_3]_0/[VOC]_0$ without the presence of NO_2. However, the introduction of NO_2 leads to a more complicated change in SOA yield, which is shown to be related to initial $[O_3]/[VOC]$ ratios. When $[O_3]_0/[VOC]_0 > 2$, the introduction of NO_2 results in an increase of SOA yield in the range of NO_2 studied in this work; whereas a weak negative effect was found for SOA formation according to the introduction of ~250 ppbv NO_2 under $[O_3]_0/[VOC]_0 < 2$ conditions. It was suggested that the effect of NO_2 on SOA formation yields from limonene ozonolysis is related to the competition between O_3- and NO_3-initiated oxidation of limonene as well as the competition between RO_2+HO_2 and RO_2+NO_2 (or NO_3). Analysis of aerosol chemical composition with Fourier-transform infrared spectroscopy (FTIR) and modeling further confirmed that the formation of peroxy acyl nitrates (PANs) and organic nitrates plays an important role in aerosol particle formation from limonene

ozonolysis at the presence of NO_2. The findings here indicate that accurately constraining SOA yields from NO_3 oxidation is essential to evaluate the influence of NO_2 on SOA formation in some real atmosphere, for example, regions with both biogenic and anthropogenic influences.

Atmos. Chem. Phys. Discuss., https://doi.org/10.5194/acp-2017-433
Manuscript under review for journal Atmos. Chem. Phys.
Discussion started: 15 June 2017

Atmospheric Chemistry and Physics Discussions

1 Introduction

Globally, biogenic volatile organic compounds (BVOCs) dominate the total emission of VOCs into the atmosphere, which are an order of magnitude more than the emissions of anthropogenic VOCs (Guenther et al., 1995). As one class of terpenoids, monoterpenes ($C_{10}H_{16}$) are estimated to account for 11% of annual BVOCs emissions, where α-pinene is the most dominant monoterpene emission on average, and limonene is also prevalent in some regions (Geron et al., 2000; Kanakidou et al., 2005; Stroud et al., 2005). Owing to their abundance in atmosphere and tendency to produce low volatile products when react with O_3, OH, and NO_3, monoterpenes contribute a major fraction of total atmospheric SOA (Guenther et al., 1995; Griffin et al., 1999; Atkinson and Arey, 2003; Ng, et al., 2017). The ozonolysis of monoterpenes, in particular, has been the focus of numerous studies for two reasons (Hoffmann et al., 1997; Griffin et al., 1999; Glausius et al., 2000; Koch et al., 2000; Iinuma et al., 2004; Leungsakul et al., 2005; Presto et al., 2005a, b; Jonsson et al., 2006; Zhang, et al., 2006; Ng et al., 2007; Saathoff et al., 2009; Pathak et al., 2012). First, reaction with ozone is a significant atmospheric sink for terpenes (Atkinson, 1997). Second, owing to the number or position difference of the double bond in molecular bone, ozonolysis of these species will contribute differently to the formation of SOA via gas-to-particle conversion (Kroll and Seinfeld 2008).

Limonene, one important monoterpene, is emitted in a major part from vegetation (Guenther et al., 1995, 2002; Griffin et al., 1999). It is the main component of essential oil extracted from citrus rind and is responsible for the strong scent of

Atmos. Chem. Phys. Discuss., https://doi.org/10.5194/acp-2017-433
Manuscript under review for journal Atmos. Chem. Phys.
Discussion started: 15 June 2017

Atmospheric Chemistry and Physics Discussions

92 oranges. Limonene is also a popular ingredient in household products, such as some
93 kinds of air fresheners and cleaners (Clausen et al., 2001; Singer et al., 2006).
94 Therefore, it is of special concern for indoor exposure considering the high production
95 of SOA and possible health risks under elevated limonene and O_3 levels (Weschler
96 and Shields, 1999; Wainman et al., 2000; Sarwar et al., 2003; Nazaroff et al., 2004;
97 Waring, 2014).

98 Limonene chemistry is especially interesting since there are two very different
99 unsaturated double bonds: endocyclic tri-substituted and exocyclic terminal. It is
100 believed that the oxidation of these double bonds, leading to the production of
101 semi-volatile and low-volatility organic compounds, results in the strong tendency of
102 limonene to form SOA. For the gas-phase reaction with ozone, it has been reported
103 that the oxidation of the endocyclic double bond (2×10^{-16} cm^3 $molecule^{-1}$ s^{-1}) occurs
104 approximately 30 times faster than for the exocyclic double bond (7×10^{-18} cm^3
105 $molecule^{-1}$ s^{-1}) (Shu and Atkinson, 1994; Zhang et al., 2006). Given the difference in
106 reaction rates, limonene is regarded as an excellent model system for multi-generation
107 SOA formation studies (Maksymiuk et al., 2009).

108 Although the formation of SOA mainly depends on the organic precursor and the
109 initiating oxidant (OH, O_3, and NO_3), it has also been shown that other factors, such
110 as NO_x (Nojgaard et al., 2006; Zhang et al., 2006; Draper et al., 2015), particle acidity
111 (Iinuma et al., 2004), relative humidity (RH) (Bonn et al., 2002; Jonsson et al., 2006,
112 2008a, b) and temperature (Jonsson et al., 2008b; Saathoff et al., 2009), can affect the
113 partitioning equilibrium of the produced semivolatile organics and influence the

reaction pathways that form SOA.

Recent studies of aromatic hydrocarbons, isoprene and terpene photooxidation, and terpene ozonolysis have demonstrated that gas-phase organic oxidation mechanisms are sensitive to NO_x (Presto et al., 2005b; Song et al., 2005; Kroll et al., 2006; Ng et al., 2007a, b; Draper et al.,2015). The effect of NO_x on the formation of SOA has been attributed primarily to the different reaction rates of organic peroxy radicals (RO_2) with nitric oxide (NO) and HO_2, and to the difference in volatilities of the products from the two respective reaction pathways (Kroll and Seinfeld, 2008). Under high-NO_x conditions, RO_2+NO dominates and results in the formation of volatile organic nitrates or fragmentation products (Presto et al., 2005b). However, the RO_2+HO_2 pathway, which is competitive in the absence of NO_x, leads to less volatile products (e.g., peroxy acids), resulting in higher SOA yields (Johnson et al., 2005; Song et al., 2007). As RO_2+NO_2 reactions have generally been considered unimportant for SOA formation due to the short lifetime of peroxy nitrates (<1 s), so-called "high-NO_x" conditions typically refer to high-NO conditions. However, Chan et al. recently suggested that greater attention should be paid to the effect of NO_2 on SOA formation (Chan et al., 2010). In their work, SOA formation from reactions between acyl peroxyl radicals and NO_2 has been found higher than that from RO_2+HO_2 reactions at sufficiently high NO_2 concentrations. Draper et al. investigated NO_2 effect on SOA formation from ozonolysis of monoterpenes at varying concentrations of NO_2 in their recent work, and they found the different NO_2 effect on the observed aerosol yields for different monoterpenes at various NO_2 levels, which is

136 essentially resulted from the competition between O_3 and NO_3 to oxidize each
137 monoterpene (Draper et al.,2015). Considering the current trend of increasing
138 tropospheric NO_2 over developing areas (i.e., East Asia) (He et al.,2007) and the high
139 NO_2 concentrations in urban indoor environments (Weschler et al., 1994; WHO, 2000;
140 Dimitroulopoulou et al., 2001), re-evaluating the effect of NO_2 on SOA formation
141 from typical atmospheric VOC oxidation is relevant to predicting aerosol production
142 in some mixed region with both biogenic and anthropogenic emissions, as well as
143 particle exposure from indoor environments and polluted urban atmospheres.

144 With respect to the critical roles of the chemical reaction mechanisms for
145 atmospheric VOCs oxidations in describing SOA formation, some explicit chemical
146 mechanisms based on experimental studies have been developed and applied to
147 describe the formation of SOA from the oxidation of anthropogenic or biogenic VOCs
148 over the years (Jenkin et al., 1997; Madronich and Calvert, 1999; Carter, 2000; Griffin
149 et al., 2002; Capouet et al., 2003; Saunders et al., 2003; Aumont et al., 2005). Among
150 these near-explicit or fully explicit chemical mechanisms, MCM describes complete
151 degradation of methane and 142 non-methane VOCs (Jenkin et al., 2015). By
152 comparison to controllable smog chamber experiments, different versions of MCM
153 have been evaluated for gas phase chemistry of alkenes (Hynes et al., 2005), isoprene
154 (Pinho et al., 2005; Jenkin et al., 2015), α- and β-pinene (Saunders et al., 2003; Pinho
155 et al., 2007; Xia et al., 2008), aromatics (Bloss et al., 2005). It seems that the use of
156 this explicit mechanism may therefore provide insight into the atmospheric oxidation
157 and the formation of SOA.

The purpose of this work is to investigate the influence of nitrogen dioxide in SOA formation following the ozonolysis of limonene. First, a systematic experimental study on the effect of NO_2 on SOA formation from limonene was conducted under varying NO_2 levels with different O_3/limonene ratios. SOA yields and mass concentration under different conditions were investigated and aerosol chemical composition was analyzed off-line with FTIR. Then the subset of MCM describing limonene ozonolysis coupled with a gas-particle partitioning model was used to simulate the NO_2 effect on SOA formation. Finally, the mechanism of the influence of NO_2 on SOA formation from ozonolysis of limonene was thoroughly analyzed by comparing experiment observations and model predictions.

2 Methods

2.1 Experimental section

All experiments were performed in a collapsible ~850 L Teflon FEP chamber, which had been used previously for characterization of oxidation of hexenols (Gai et al., 2015), SOA from photooxidation of aromatic organic hydrocarbons (Huang et al., 2013), and vacuum ultraviolet photoionization mass spectra of isoprene photooxidation products (Pan et al., 2012). Briefly, the chamber was irradiated with UV light (300-400 nm) overnight and flushed with dry zero air until the background particle number less than 10 cm^{-3} prior to each experiment. A known volume of limonene was firstly injected into a 250 mL temperature-controlled glass bulb vaporizer (298-598K), and then flushed into the smog chamber with purified air (4 L/min) for about 20 min, the concentration of which was monitored with a gas

chromatograph- flame ionization detection (GC-FID, Agilent 7820) during the whole experiment. Typically, excessive 2-butanol was also introduced into the smog chamber as OH scavenger to suppress the influence of OH radicals produced from the O_3-limonene reaction. To investigate the effect of NO_2, a certain concentration of mixture of NO_2/purified air was pumped into the main reactor using a 0.4 L/min miniature vacuum pump. The appropriate concentration of NO_2 inside the chamber was obtained by controlling the pumping time, and monitored with NO_x analyzer (TEI model 42i). Ozone was produced with an ozone generator in a 1 L/min clean air stream, and the oxidation of precursors inside the reactor was initiated by the introducing of O_3. The O_3 concentration inside the chamber was measured in real time by O_3 analyzer (TEI model 49i). Aerosol produced from the limonene/O_3 system under various NO_2 concentrations was monitored on-line with a scanning mobility particle sizer (SMPS, TSI, 3936, USA) consisting of a differential mobility analyzer (DMA, TSI model 3080) and a condensation particle counter (CPC, TSI model 3775). To investigate the chemical composition of SOA, particle products were also collected with PTFE filters (Pall Life Sciences, USA) for off-line FTIR analysis in some experiments. Detailed information on the chemicals and off-line FTIR analysis of aerosol is provided in the Supplement.

2.2 Model description

To obtain insight into the effect of NO_2 on SOA formation from limonene, MCM coupled with a gas-particle partitioning model was applied against smog chamber experiments. The current 3.3.1 version of MCM (Jenkin et al., 2015), available online

Atmos. Chem. Phys. Discuss., https://doi.org/10.5194/acp-2017-433
Manuscript under review for journal Atmos. Chem. Phys.
Discussion started: 15 June 2017

Atmospheric Chemistry and Physics Discussions

(*http://mcm.leeds.ac.uk/MCM*), represents the degradation of methane and 142 non-methane VOCs. The subset of MCM v3.3.1 describing limonene and 2-butanol oxidation, containing 2272 chemical reactions and 749 compounds, was chosen for gas phase species evaluation in this work.

The gas-particle partitioning mechanism was first proposed by Pankow (Pankow, 1994a,b) and has been widely used to describe the formation of organic aerosols. In principle, products from oxidation of VOCs described in MCM or the other chemical mechanisms can partition between the gas phase and the particle phase according to their corresponding saturation vapor pressure (p_L^o). By means of the online facility UManSysProp (Topping et al., 2016), the applied p_L^o values of each stable species were predicted using the EVAPORATION method (Compernolle et al., 2016). For comparison, the saturation vapor pressures in this work were calculated at 291 K or 298 K according to the experiment conditions. Based on the ideal gas and Raoult's law, the partitioning coefficient $K_{p,i}$ (m^3 μg^{-1}), which defines the thermodynamic equilibrium of a given organic species between the gas and particle phases, can be determined from Eq.(1):

$$K_{p,i} = \frac{760RT}{10^6 \bar{M}_{om} \gamma_i p_{L,i}^0} \quad (1)$$

where R is ideal gas constant (8.026×10^{-5} m^3 atm mol^{-1} K^{-1}), T is temperature (K), $\bar{M}_{om}$ is the average molecular weight of organic matter (g mol^{-1}), γ_i is the activity coefficient of compound i and set to be 1 (assumed as ideal thin solution), and $p_{L,i}^0$ is the saturation vapor pressure of i. Then A_g (gaseous concentration) and F_{om} (particulate-associated concentration) can be determined according to F_{om}/A_g =

Atmos. Chem. Phys. Discuss., https://doi.org/10.5194/acp-2017-433
Manuscript under review for journal Atmos. Chem. Phys.
Discussion started: 15 June 2017

Atmospheric Chemistry and Physics Discussions

$K_p \cdot TSP$, where *TSP* is the mass concentration of total suspended particulate material (in μg m^{-3}).

It is assumed that equilibrium partitioning can be achieved instantaneously; therefore, no chemical processes in the aerosol phase were considered in model simulations in this work. Generally, it is believed that compounds with more carbons are likely to condense into the aerosol phase without consideration of oligomers that exist in the aerosol phase (Seinfeld and Pandis, 1998; Xia et al., 2008). In this work, 385 stable species with more than three carbons, out of the 701 organic compounds, were included for gas-particle partitioning simulation for oxidation of limonene.

3 Results and discussion

As listed in Table 1, 21 darkened chamber experiments were carried out at room temperature to investigate the influence of NO_2 on SOA formation in the ozonolysis of limonene, which can be classified into three scenarios according to the corresponding experimental conditions. In the first, ozonolysis of limonene was studied under various $[O_3]_0/[VOC]_0$ ratios without NO_2. In the second scenario, ozonolysis of limonene was investigated with ~ 250 ppbv $[NO_2]_0$ under various $[O_3]_0/[VOC]_0$ ratios. In the third scenario, the influence of NO_2 on SOA yield was further explored under a constant $[O_3]_0/[VOC]_0$ ratio ($[O_3]_0/[VOC]_0$ ~2.4). During each run, temperature and RH were kept almost constant. For all these experiments, no inorganic seeds were added. Despite the fact that the effect of vapor wall loss on SOA formation yield may be constrained by introducing seed aerosol to promote the condensation of SOA-forming vapors on it, it is found that the effect can also be

Atmos. Chem. Phys. Discuss., https://doi.org/10.5194/acp-2017-433
Manuscript under review for journal Atmos. Chem. Phys.
Discussion started: 15 June 2017

mitigated for the reaction system with fast oxidation rate (Nah et al., 2016). Regarding the high rate coefficient of limonene ozonolysis and $[O_3]_0/[VOC]_0$ ratio >2 in most experiments in this work, and even for $[O_3]_0/[VOC]_0$ ratio ≤ 2 cases, the main focus is to learn the effect of NO_2 on SOA formation, it is presumed that the effect of vapor wall loss does not affect the conclusions of the article. An averaged aerosol density of 1.3 g cm^{-3} was chosen to calculate the total mass of SOA formation from limonene ozonolysis from the total measured aerosol volume by SMPS (Wirtz and Martin-Reviejo, 2003; Saathoff et al., 2009).

The model based on the subset of MCM describing limonene ozonolysis was compared to the experimental data. In general, all the initial conditions for model simulations follow the experimental conditions, and the total simulation time in model was equal to the duration of the smog experiments.

Table 1

3.1 Gas-phase reaction

Figure 1 shows the time evolution of the ozone mixing ratio, NO_2 level, the precursor limonene concentrations, as well as SOA formation from experimental observations and model predictions in a typical high-NO_2 and high-O_3 experiment (Exp.N19). The box model studies based on the subset of the MCM for ozonolysis of limonene reasonably describe most of the experimental gas-phase species concentration profiles in this work. The substantial agreement between the model-predicted and the experimentally observed precursor limonene shows that limonene decays very rapidly following the initiation of the reaction and is depleted in

268 the first 30 minutes. The simulation also performs well in predicting changes in NO_2
269 during the reaction. Although both the predicted and observed results show roughly
270 similar temporal profiles, the simulation overpredicts O_3 by approximately 30% for all
271 data after 30min. Different from the evolution of precursor limonene, NO_2 and O_3
272 keep slowly decreasing, and SOA mass concentrations also keep increasing after the
273 first rapid reaction period, which suggests multi-step reactions leading to particle
274 formation.

275 Similar to this work, previous chamber simulation studies in other groups have
276 also shown the difficulty of predicting O_3, and under- or over-predictions appeared in
277 different cases (Chen et al., 2005; Yarwood et al., 2005; Xu et al., 2015). Although
278 the main reason resulting in the discrepancy between experimental and simulated O_3
279 concentration in this work needs further study, for simulating the formation of
280 limonene-derived SOA in this study, the performance of the model is qualitatively
281 acceptable in simulating gas-phase species (especially for precursor limonene).

282 **3.2 NO_2 effect on SOA yield**

283 **3.2.1 Chamber experiments of limonene/O_3 system in the absence or presence**
284 **of NO_2**

285 To investigate the effect of NO_2 on the limonene/O_3 system, 16 experiments
286 (N1-N16) were conducted under two typical NO_2 scenarios: low NO_2 (<1 ppbv, minor
287 NO_2 is presumed to be produced concomitantly with the generation of O_3 from
288 corona-discharge) and high NO_2 (236.7-293.4 ppbv), where the initial limonene
289 mixing ratios are approximately the same (~ 125 ppbv) under the various O_3

Atmos. Chem. Phys. Discuss., https://doi.org/10.5194/acp-2017-433
Manuscript under review for journal Atmos. Chem. Phys.
Discussion started: 15 June 2017

Atmospheric Chemistry and Physics Discussions

concentrations. According to the partitioning theory originally outlined by Pankow (Pankow, 1994a, b) and Odum et al.(Odum et al. 1996), SOA yields are calculated from the ratio of the amount of SOA formed (ΔM_0, $\mu g/m^3$, after correction of wall losses, see in supplement) to the amount of hydrocarbon consumed (ΔHC, $\mu g/m^3$),

$$Y = \frac{\Delta M_0}{\Delta HC} \quad (1)$$

As listed in Table 1 and shown in Figure 2, the results show two striking features. In the absence of NO_2 (N1-N7), SOA yields (black squares in Figure 2) increase smoothly with increasing initial O_3 concentration at almost the same $[VOC]_0$, which indicates the contribution of the different generation products according to the extents of limonene ozonolysis to SOA formation (Ng et al., 2006). In the presence of NO_2, however, change in SOA yields becomes more complicated (N8-N16, red circles in Figure 2). It is shown that at $[O_3]_0/[VOC]_0 < 2$ conditions (N8-N12), the introduction of NO_2 results in a weak negative effect on the SOA yields compared to that without NO_2. While at $[O_3]_0/[VOC]_0 > 2$ conditions (N13-N16), SOA yields increase substantially, far exceeding those without NO_2 at a similar mixing ratio of $[O_3]_0$ and $[limonene]_0$ following the introduction of NO_2 in the reaction system. And this increase cannot be attributed simply to the increase of initial O_3 concentration in comparison to the experimental results of N4-N7. It seems that NO_2, entangled with the initial O_3 concentration, participates in some key reaction pathways of limonene/O_3 system influencing SOA formation.

Figure 2

3.2.2 NO_2 experiments under a constant $[O_3]_0/[VOC]_0$ ratio with excess O_3

Atmos. Chem. Phys. Discuss., https://doi.org/10.5194/acp-2017-433
Manuscript under review for journal Atmos. Chem. Phys.
Discussion started: 15 June 2017

Atmospheric Chemistry and Physics Discussions

312 To further investigate the effect of NO_2 on SOA formation in the limonene/O_3
313 reaction system，the third group of experiments (N17-N21) were conducted by adding
314 different concentrations of NO_2 to limonene/O_3 at the beginning of the experiments,
315 while the $[O_3]_0/[VOC]_0$ ratio was kept roughly constant ($[O_3]_0/[VOC]_0$ =2.5). In these
316 experiments, limonene completely reacted (~122 ppbv) due to high O_3 concentration
317 (~300 ppbv).

318 As shown in Figure 3, given the similar relative humidity (14.4% ± 0.6%),
319 temperature (25.6 ± 0.6 ℃), initial limonene concentration (122.2 ± 3.2 ppbv), and
320 initial ozone concentration (~300 ppbv), aerosol formation increases as NO_2 added to
321 the system increases. At relatively low NO_2 concentrations (<200 ppbv), the SOA
322 yield and mass concentration were found to increase rapidly with increasing NO_2;
323 whereas the rate of increase tends to slow as the initial NO_2 concentration added
324 exceeds 300 ppbv. Given the constant $[O_3]_0/[VOC]_0$ ratio with excess O_3, both particle
325 concentration and particle size increase with the NO_2 level progressively, e.g., the
326 mode diameter increases from 95 to 107 nm and the total concentration increases from
327 1.77×10^5 to 2.17×10^5 particles/cm^3 by adding 298.5 ppbv NO_2 (Figure S2 in
328 supplement).

329 **Figure 3**

330 SOA formation form limonene ozonolysis has also been examined by Zhang et al.
331 under different NOx (NO + NO_2) levels and O_3 levels (Zhang et al., 2006). It was
332 found that heterogeneous oxidation of the first-generation products by ozone uptake
333 on unsaturated SOA particles are rate-limiting at low NOx, while at high NOx,

gas-phase ozonolysis of the terminal double bond dominates. As shown in Figure S3, the SOA yields under high ratios of ozone-to-limonene (>> 10) without NOx in their work is far higher than that observed in this work, which indicates the heterogeneous oxidation of the exo bond follow immediately the initial oxidation of endo double bond. Donahue et al. have explored SOA formation from ozonolysis of limona ketone, a potentially important intermediate in limonene ozonolysis (Donahue et al., 2007). And it was found that SOA formation from limona ketone is similar to that from a-pinene, but a factor of four less intense than from limonene at low ozone-to-limonene ratio (<1) (see the lower dashed line in Figure S3). It seems that SOA yields from limonene + ozone of this work fall into the range between the two aforementioned work, indicting the dependence of SOA formation on the level of multigenerational oxidation of limonene that can occur. At the presence of NO_2, the trend of SOA yields is more complex due to differences in the volatility of the entire product suite formed from different reaction passways. These sensitivities to ozone-to-limonene ratio and NOx suggest that great care should be taken in extrapolating laboratory results to real atmosphere.

3.2.3 Comparison of model-predicted SOA yields with experimentally observed yields

To explore the NO_2 effect on SOA formation during the ozonolysis of limonene, the simulated SOA yields were explored under different NO_2 conditions, which were further compared with the experimental data. Figure 4 shows the dependence of SOA yield (both observed and predicted) on NO_2 level, as well as O_3 level, for oxidation of

limonene. Reasonable agreement is shown between the trend of the predicted SOA yields and the experimentally observed results according to the change of NO_2, which indicates that the MCM /gas-aerosol partitioning model adequately captures the effect of NO_2 on SOA yield for the limonene/O_3 reaction system. For example, the model-predicted SOA yields tend to increase explicitly with increasing initial O_3 concentrations with (Exp N8-N16 series) or without NO_2 (Exp N1-N7 series), consistent with the experimental results discussed in 3.2.1. As for the constant $[O_3]_0/[VOC]_0$ ratio with excess O_3, the predicted SOA yields, increasing with increasing $[NO_2]_0$, are roughly equal to the observed SOA yields except at 611 ppbv $[NO_2]_0$, where the predicted SOA yield is less than the observed value. It is noteworthy that the two different temperatures were used for model simulation in Figure 4 (N1-N16:291K; N17-N21:298K) according to the experimental conditions. As the slope of the fit line is 1.4, it means that the predicted results are higher than the observed ones. It also can be found that the predicted yields at the lower temperature are far higher than that at higher temperature (see comparison in Figure S4 in supplement). SOA formation from ozonolysis of limonene has been investigated as a function of temperature in the range of 253–313 K, and negative dependence of SOA yields on temperature has been found (Saathoff et al., 2009). Based on their work and the corresponding organic aerosol mass in this work, 15% increase of SOA yields at the utmost can be attributed to the 7 K temperature difference between Exp.N1-N16 and N17-N21. However, the predicted yields at 291K(N1-N16) is 1.5 to 2 times of that at 298K(N1-N16) (Figure S4 in supplement), it is presumed that this big

difference maybe result from the imprecise evaluation for the saturation vapor pressures of the different kind of products of limonene ozonolysis.

Figure 4

The sensitivity of the SOA yield to NO_2 and O_3 was explored further based on 861 simulations, with the concentration of O_3 ranging from 0 to 800 ppb and NO_2 ranging from 0 to 400 ppb, while the initial concentration of limonene was set as 125 ppb, close to the typical concentration of limonene adopted in the chamber experiments in this work (See Table 1). Figure S5a in supplement shows the simulated SOA yield as a function of O_3 and NO_2 level at 291K. Most SOA yields here refer to the yields when >90% of initial limonene loading was consumed. Generally, higher yields can be observed for higher O_3 level or NO_2 level as aforementioned. As shown in Figure S5b, at the two typical NO_2 concentrations (0.1 and 0.26 ppm similar to the experimental conditions), the simulated SOA yields show a positive correlation with the initial O_3 concentrations no matter the concentration of NO_2, which is consistent with the experimental trend. However, the relationship between the SOA yields and the initial NO_2 levels are more complicated and entangled with O_3 concentration. As shown in Figure S5c, in the presence of 100 ppb O_3, the simulated SOA yield first deceases with increasing NO_2 at low concentration (below 50 ppb). This may qualitatively explain the experimental observation that SOA yields in the presence of NO_2 are smaller than those in the absence of NO_2 under $[O_3]_0/[VOC]_0 < 2$ conditions, as shown in Figure 2. Then the simulated SOA yield increases with increasing NO_2 at the moderate region (ranging from 0.05 to 0.3 ppmv), and finally decreases again with

400 increasing NO_2 when concentrations are even higher. In the presence of 300 ppbv O_3,
401 simulated SOA yields show an increasing trend with increasing NO_2 until
402 approximately 0.3 ppmv, and a decreasing trend with increasing NO_2 after this point.
403 For comparison, the experimental data of N17-N20 and the model predicted results at
404 298K, where $[O_3]_0$ was equal to the simulation conditions (~300 ppbv), are also
405 shown in Figure S4c. It is obvious to see the difference resulting from the predictions
406 in different temperatures. In the presence of even higher O_3 (0.7 ppmv here), the
407 simulated SOA yield first increases and then levels off with increasing NO_2.

408 **3.3 NO_2 effect on SOA chemical components**

409 **3.3.1 FTIR analysis of SOA particles formation in the limonene/O_3 system**

410 Traditionally, the effect of NO_x on SOA formation was believed to result from the
411 competition between the reaction of RO_2+HO_2 and that of RO_2+NO. The RO_2+HO_2
412 pathway, which dominates at low NO_x condition, tends to produce less volatile
413 organic hydroperoxides (ROOHs) and peroxy acids, leading to the formation of SOA.
414 Under high-NO conditions, the reaction of RO_2 with NO will result in the production
415 of volatile organic nitrates. However, this reaction pathway can be ruled out at high
416 O_3 conditions. Although RO_2+NO_2 reactions have been considered less important
417 before for SOA formation, it was confirmed recently that the formation of peroxy acyl
418 nitrates (PANs, $RC(O)OONO_2$) contribute certainly to SOA formation from the
419 oxidation of sesquiterpenes (Ng et al., 2007) and aldehydes (Chan et al., 2010) at high
420 NO_2 levels. While in the recent literature, reactions of NO_3 with BVOCs have
421 received increased attention and been recognized as a potential source of SOA from

ozonolysis of BVOCs at high NO_2 concentration (Ng et al., 2017).

To learn the effect of NO_2 on the SOA chemical component, the filtered particle-phase products from the chamber limonene/O_3 reaction were analyzed by FTIR. Here, the FTIR spectra of particles separately collected from high NO_2 experiment (~660 ppbv) and low NO_2 experiment (<1 ppbv), as well as the spectra for a blank PTFE filter, are shown in Figure 5. Compared with the base absorption spectrum, the samples from oxidation of limonene feature absorption at 1720 cm^{-1}, which indicates the production of compounds with a carbonyl group, such as aldehydes, ketones, or acids (Leungsakul et al., 2005; Presto et al., 2005b). Disparate features are evident in the IR spectra of high-NO_2 experiment as compared with no-NO_2 experiment. Following previous experimental works (Presto et al., 2005b; Palen et al. 1992; Bruns et al., 2010) and field work (Mylonas et al. 1991), these features are assigned as characteristic organic nitrate IR peaks, according to NO symmetric stretch (860 cm^{-1}), NO_2 symmetric stretch (1280 cm^{-1}) and NO_2 asymmetric stretch (1630-1640 cm^{-1}) (Socrates et al. 2001).

Figure 5

FTIR analysis of SOA particles in this work has identified the contribution of organic nitrates to SOA formation in limonene/O_3 system in the presence of high NO_2. Actually, the contribution of low-volatility organic nitrate to total particle mass has also been observed in the SOA formation from limonene ozonolysis (Zhang et al., 2006) or photooxidation of sequiterpenes (such as longifolene and aromadendrene) (Ng et al., 2007) at the presence of NO_x. Recently, organic nitrate in SOA formation

from ozonolysis of limonene has been evaluated at varying concentration of NO_2, and the organic nitrate yield from NO_3 + limonene is found to be about 30% (Fry et al., 2011; Draper et al., 2015). Regarding to the similar reaction conditions to the work in Fry et al. and Draper et al., organic nitrate observed here is suggested to be resulted from direct NO_3 oxidaition of limonene or indirect NO_2/NO_3 reaction with the reactive intermediate compounds following ozonolysis of limonene.

3.3.2 Model results of the NO_2 effect on total SOA

As mentioned, our FTIR analysis of SOA particles has confirmed that compounds with carbonyl groups contribute to the particle phase regardless of the presence of NO_2, while organic nitrates contribute to the particle phase only in the presence of NO_2. To evaluate the effect of NO_2 on aerosol formation, simulation work was also carried out based on MCM model. The total mass (unit: μg m^{-3}) of the four groups of main products (ROOHs, acids, PANs, and nitrates (PANs are excluded)) in both gas and aerosol phases with the five typical different initial mixing ratios of NO_2 are predicted at the assumed conditions of 125 ppbv $[limonene]_0$, 300 ppbv $[O_3]_0$ and 291K.

As shown in Figure 6, both the total mass (gas phase + aerosol phase) of ROOHs and of acids decrease with increasing NO_2, which is interpreted with the recognized mechanism of RO_2+HO_2 reaction (Johnson et al., 2005). However, their relative proportions to gas phase and aerosol phase show different trends following changes in NO_2 concentration. It is obvious that in gas phase, the relative proportion of ROOHs decreases very fast with increasing NO_2; while in aerosol phase, ROOHs increases

slightly when NO_2 increases from 0.0 ppmv to 0.1 ppmv; and then decreases slowly with increasing NO_2. Even in high NO_2 conditions, ROOHs still mostly contribute to organic aerosols. While the fraction of acids decease monotonically both in gas phase and aerosol phase. Given its high volatility, it is obvious that PANs increase greatly in the gas phase with increasing NO_2. Considering that the increase of PANs in the gas phase in turn increases its partitioning into the particle phase, it is reasonable to suggest that PANs may also contribute its proportion to organic aerosol. In this simulation work, PANs show the same trends both in the gas phase and aerosol, first increasing with increasing NO_2 from 0.1 ppmv to 0.3 ppmv, and then decreasing slowly with increasing NO_2. As shown in Figure 6b, the particle phase PANs contribute the second proportion to total particle compounds. Organic nitrates increase both in gas and particle amount with the increase of NO_2, too. And the particle phase nitrates, which are also believed to result from increased partitioning, contribute the third proportion to total particle compounds.

Regarding the model conditions, for example, 125 ppbv $[limonene]_0$ and 300 ppbv $[O_3]_0$, the contributions of ROOHs, acids, PANs and organic nitrates to particle phase according to the changing of NO_2 concentration appear to result in a corresponding changing trend of SOA yield with changing NO_2 (see Figure S5c). The simulation result here also gives a semi-qualitative explanation for the FTIR analysis of SOA particles.

Figure 6

3.3.3 Model Investigation of SOA Chemical Composition by Individual Product

488 **Species**

489 Although 385 condensable compounds have been examined in this simulation,
490 most contribute negligible fractions to total aerosol mass. By assessing the
491 corresponding aerosol mass fractions at 5 different NO_2 scenarios, the 20 dominant
492 condensable compounds were identified. As summarized in Table 2, most of these
493 compounds have carbon numbers larger than seven, with the two exception of
494 C628OOH (a six-carbon compound) and C735OOH (a seven-carbon compound),
495 which confirmed that organic compounds with more than six carbons have major
496 potential to form SOA (Seinfeld and Pandis, 1998). As shown in Table 2, 10 of the 20
497 dominant condensable compounds are ROOHs, and the rest include 4 acids, 3 PANs
498 and 3 nitrates. Their relative aerosol mass fractions to total SOA mass at different
499 initial concentrations of NO_2 are shown in Figure 7. Across all simulations at five
500 different NO_2 scenarios, the selected 20 dominant condensable compounds cover
501 93-96% of the total SOA mass. The simulation results indicate that most of the
502 individual compounds follow the same pattern for the grouped compounds as
503 illustrated in Figure 6b. Most of the ROOHs and acids contribute more to the total
504 SOA mass at low NO_2 conditions, while their relative importance significantly
505 decreases with increasing NO_2. On the contrary, the relative contributions of the most
506 PANs and nitrates to total SOA increase with increasing NO_2. It is interesting to note
507 some exceptions. Both NLIMOOH(C10H17NO5) and NLIMALOOH (C10H17NO7)
508 are ROOHs, and their mass fractions increase as the NO_2 concentration increases. In
509 particular, NLIMOOH has an aerosol mass fraction above 50% relative to the total

SOA mass when NO_2 concentration is higher than 0.2 ppmv. Although NLIMOOH and NLIMALOOH are ROOHs, the two compounds also contain an -ONO_2 group in the molecular blocks (see Table S1). Detailed reaction pathway analysis (in the following 3.4 section) show that their production are related to NO_3 reactions, so it is reasonable to find their mass fractions increasing with increasing NO_2. For C823PAN(C9H13NO7), the result is opposite, its mass fraction decreases rather than increases with increasing NO_2. Although it is traditionally attributed to PANs, C823PAN also has a carboxyl group (C(O)OH). The reaction pathway analysis (in the following 3.4 section) show its production are related to RO_2+NO_2 reactions, which maybe explain why its trend changes with changing NO_2.

Figure 7

3.4. Reaction pathway analysis

To understand the relationship between SOA yield and NO_2 level, as well as the individual aerosol compositions and NO_2 level, the mechanism of oxidation of limonene by O_3 in the presence of NO_2 should be considered comprehensively. As shown in Scheme 1, NO_2 can affect SOA formation from ozonolysis of limonene in two different ways: it can form NO_3 firstly (Atkinson, 1997) that can compete with O_3 to oxidize limonene directly, or react with RO_2 radicals or other products and reaction intermediates as NO_2 or NO_3.

Scheme 1

Although a few of work reported that the nucleation potential of O_3 is much higher than that of NO_3 (Bonn et al., 2002; Nojgaard et al., 2006), there are more

532 laboratory and chamber studies suggested that NO_3- BVOC chemistry is a potentially
533 efficient SOA formation mechanism, and some SOA yield from NO_3 oxidation of
534 terpenes are even greater than that for OH or O_3 oxidation (Ng et al., 2017). The
535 model study here confirmed that the reaction of NO_3 with limonene at elevated NO_2
536 and O_3 plays an important role in the formation of SOA. Firstly, the initial
537 competition between O_3 and NO_3 oxidation directly results in distinct decrease of
538 ROOHs and acids with the increasing NO_2. Secondly, NO_3- initiated oxidation of
539 limonene itself can also produce some condensable compounds contributing to SOA
540 formation. For example, both NLIMOOH, the largest contributor to the total SOA
541 mass, and the other dominant condensable compound LIMBNO3 are products from
542 NO_3+limonene reaction passage (Figure 7). In fact, large amounts of yet unidentified
543 organic nitrates (approximately 30%) have also been found experimentally as the
544 major reaction product of limonene oxidation by NO_3 (Spittler et al., 2006; Fry et al.,
545 2011), which substantiates the observation in this work.

546 NO_2 effect on SOA formation is embodied not only in the initial competition
547 between O_3 and NO_3 oxidation, but also in participation in the production of PANs
548 and nitrates following ozonolysis of limonene. The first step of limonene ozonolysis is
549 dominated by cycloaddition of O_3 to the endocyclic double bond (Leungsakul et al.,
550 2005; Pan et al., 2009). Two highly reactive Criegee intermediates (CI*, named
551 LIMOOA and LIMOOB here) are produced following the breakage of limonene's
552 cyclohexene ring. However, subsequent reactions of the CIs involve various reactions
553 with RO_2 or HO_2, as well as NO_2 or NO_3 (see details in Scheme S1 and Scheme S2 in

supplement), which will affect the formation of SOA. For example, production of C822PAN (a C9 PAN) and C822CO2H (a C9 acid) is involved in the competition between the reactions of C822CO3 (a C9 peroxy radical as an intermediate product of LIMOOA) with RO_2/HO_2 and with NO_2. While LIMONIC (abbreviation for limonic acid, See Table 2), one main aerosol component identified experimentally (Walser et al., 2008) and theoretically (Pathak et al., 2012), and C823PAN are also related to the competition between the reactions of C823CO3 (another C9 peroxy radical with a carboxyl) with RO_2/HO_2 and with NO_2. In the following reactions related to LIMOOB, LIMBOO (stabilized form of LIMOOB) tends to react with H_2O in the absence of NO_2, leading to the formation of limononic acid (abbreviated as LIMONONIC, See Table S1), one of the main identified aerosol-phase acids (Pathak et al., 2012; Walser et al., 2008). While in the presence of NO_2, LIMBOO will react with NO_2 to produce limononaldehyde firstly (abbreviated as LIMAL here), which is followed with multiple reactions leading to the formation of a series of condensable compounds. For example, reaction of LIMAL with RO_2 will also form LIMONONIC. Whereas multi-step reactions of LIMAL with NO_3 will lead to the generation of NLIMALOH and C817PAN, two dominant contributor to particle mass as listed in Table 2 and shown in Figure 7. Considering the competitions between the different reaction pathways related to $NO_2(NO_3)$ and $RO_2(HO_2)$, it is reasonable to see the different profile of the various reaction products contributing to aerosol mass according to the different NO_2 levels as discussed in part 3.3.3 and shown in Figure 7.

4 Conclusions

This work has systematically investigated the effect of NO_2 on SOA yields and composition from ozonolysis of limonene. Although the concentrations for the gaseous compounds of interest (limonene, NO_2 and O_3) in real atmosphere is not exactly same to precursor concentrations used in this work, and the chemistry in real atmosphere is also more complicated than that in smog chamber and box model studied here, thus absolute observed aerosol yields are not atmospherically relevant directly. That the ratios of $[NO_2]_0$: $[limonene]_0$ are approximately 2 : 1(Exp.N8-N16) and $[NO_2]_0$: $[O_3]_0$ range from 3.7 : 1 to 0.4 : 1 (Exp. N8-N21 except) are reasonable for relatively polluted while with high BVOCs emission sites in the real atmosphere or some indoor conditions.

Both experimental observation and model prediction have demonstrated that the effect of NO_2 on the formation of SOA from a limonene/O_3 reaction mixture is more complicated than previously acknowledged. Analysis of the reaction pathway and the related aerosol chemical composition suggests that NO_2 is not only related to the initial competition between O_3 and NO_3 oxidation of limonene, but also the competition between RO_2+HO_2 and RO_2+NO_2(or NO_3) following the ozonolysis of limonene. The important role of peroxy acyl nitrates (PANs) and organic nitrates, in addition to ROOHs and acids, have been identified in aerosol particle formation from limonene ozonolysis with the presence of NO_2. And fractions relative to the total SOA mass from PANs, organic nitrates, ROOHs and acids have been found sensitive to the change of the $[O_3]_0/[VOC]_0$ ratios and $[NO_2]_0$: $[VOC]_0$ ratios.

Actually, understanding the effects of anthropogenic emissions on aerosol

598 formation from biogenic emissions and to answer to what extent can biogenic SOA be
599 controlled is a critical area whenas a challenge of current research (Ng et al., 2017). In
600 a series recent field campaigns carried in the U.S. (Rollins et al., 2012; Setyan et al.,
601 2012; Fry et al., 2013; Xu et al., 2015a, 2015b) and in Europe (Kulmala et al., 2011;
602 Crippa et al., 2013; Hao et al., 2014; Kiendler-Scharr et al., 2016), organic nitrates are
603 found ubiquitous in SOA formed from the reaction of nitrate radicals (NO_3) and
604 BVOCs. For example, Xu et al. studied the effect of anthropogenic NOx on biogenic
605 aerosol formation in the southeastern US, and found that monoterpenes+NO_3
606 chemistry accounts for 50% of total nighttime OA production (Xu et al., 2015a), and
607 organic nitrates can contribute 63-100% of total nitrates in the southeastern US (Xu et
608 al., 2015b). As in a recent field campaign carried in Europe, organic nitrates were
609 found to contribute one-third of the total nitrate mass in a boreal forestland–urban
610 mixed region, and the formation of organic nitrates was also suggested as the outcome
611 of BVOCs undergoing nighttime chemistry with NO_3 (Hao et al., 2014), which
612 confirmed the findings in other location in Europe (Kiendler-Scharr et al., 2016).
613 Considering their measurement site is influenced by both biogenic and anthropogenic
614 sources, similar to the situations researched in this work, their observation confirmed
615 the suggestions in this work that the effect of NO_2 on SOA yields from
616 atmospherically relevant BVOCs, especially under the complex atmosphere with high
617 O_3 and NO_2, should be evaluated more systematically than before, and more work are
618 needed in order to more accurately treat aerosol formation for regions with substantial
619 anthropogenic-biogenic interactions and predict air quality and climate.

Acknowledgements. The authors gratefully acknowledge support from the National Natural Science Foundation of China (41575126, U1532143, 91544228, 41575125, 41375147, 41575118, U1232209).

Supporting Information

Chemicals, experimental details for off-line FTIR analysis, correction for SOA wall loss, Figures S1–S6 and Scheme S1-S2 are available in the Supporting Information.

References

Atkinson, R.: J. Phys. Chem. Ref. Data, 26, Monograph 1, 1997.

Atkinson, R. and Arey, J.: Gas-phase tropospheric chemistry of biogenic volatile organic compounds: a review, Atmos. Environ., 37, Supplement No. 2, S197–S219, 2003.

Aumont, B., Szopa, S., and Madronich, S.: Modelling the evolution of organic carbon during its gas-phase tropospheric oxidation: development of an explicit model based on a self generating approach. Atmos. Chem. Phys., 5(9), 2497–2517, 2005.

Bloss, C., Wagner, V., Bonzanini, A., Jenkin, M. E., Wirtz, K., Martin-Reviejo, M., and Pilling, M. J.: Evaluation of detailed aromatic mechanisms (MCMv3 and MCMv3.1) against environmental chamber data. Atmos. Chem. Phys., 5, 623–639, 2005a.

Bloss, C.; Wagner, V.; Jenkin, M. E.; Volkamer, R.; Bloss, W. J.; Lee, J. D.; Heard, D. E.; Wirtz, K.; Martin-Reviejo, M.; Rea, G.; Wenger, J. C.; and Pilling, M. J.: Development of a detailed chemical mechanism (MCMv3.1) for the atmospheric

642 oxidation of aromatic hydrocarbons, Atmos. Chem. Phys., 5, 641–664, 2005b.

643 Bonn, B., and Moortgat, G. K.: New particle formation during α- and β-pinene
644 oxidation by O_3, OH and NO_3, and the influence of water vapour: particle size
645 distribution studies, Atmos. Chem. Phys., 2, 183–196, 2002a.

646 Bonn, B., Schuster, G., and Moortgat, G. K.: Influence of water vapor on the process
647 of new particle formation during monoterpene ozonolysis, J. Phys. Chem. A, 106,
648 2869–2881, 2002b.

649 Bruns, E. A., Perraud, V., Zelenyuk, A., Ezell, M. J., Johnson, S. N., Yu, Y., Imre, D.,
650 Finlayson-Pitts, B. J., and Alexander, M. L.: Comparison of FTIR and particle
651 mass spectrometry for the measurement of particulate organic nitrates. Environ.
652 Sci. Technol., 44, 1056–1061, 2010.

653 Capouet, M., Müller, J. F., Ceulemans, K., Compernolle, S., Vereecken, L., and
654 Peeters, J.: Modeling aerosol formation in alpha-pinene photo-oxidation
655 experiments. J. Geophys. Res., [Atmos.], 113(D2), D02308,
656 doi:10.1029/2007JD008995, 2008.

657 Carter, W. P. L.: Development and evaluation of the SAPRC-99 chemical mechanism,
658 Rep. 00-AP-RT17-001-FR, 2000, Air Pollut. Res. Cent. and Coll. of Eng. Cent.
659 for Environ. Res. and Technol., Univ. of Calif., Riverside, Calif.

660 Ceulemans, K.; Compernolle, S.; Peeters, J.; Müller, J. F. Evaluation of a detailed
661 model of secondary organic aerosol formation from α-pinene against dark
662 ozonolysis experiments. Atmos. Environ., 44(40), 5434–5442, 2010.

663 Chan, A. W. H., Chan, M. N., Surratt, J. D., Chhabra, P. S., Loza, C. L., Crounse, J.

664 D., Yee, L. D., Flagan, R. C., Wennberg, P. O., and Seinfeld, J. H.: Role of
665 aldehyde chemistry and NO_x concentrations in secondary organic aerosol
666 formation. Atmos. Chem. Phys., 10, 7169–7188, 2010.
667 Chen, J., and Griffin, R. J.: Modeling secondary organic aerosol formation from
668 oxidation of a-pinene, b-pinene, and d-limonene, Atmos. Environ., 39, 7731–7744,
669 2005.
670 Clausen, P. A., Wilkins, C. K., Wolkoff, P., and Nielsen, G. D.: Chemical and
671 biological evaluation of a reaction mixture of R-(+)-limonene/ozone. Formation of
672 strong airway irritants. Environ. Int., 26, 511–522, 2001.
673 Compernolle, S., Ceulemans, K., Müller, J. F.: EVAPORATION: a new vapour
674 pressure estimation method for organic molecules including non-additivity and
675 intramolecular interactions, Atmos. Chem. Phys.,11(18), 9431–9450, 2011.
676 Crippa, M., Canonaco, F., Lanz, V. A., Äijälä, M., Allan, J. D., Carbone, S., Capes,
677 G., Ceburnis, D., Dall'Osto, M., Day, D. A., De-Carlo, P. F., Ehn, M., Eriksson,
678 A., Freney, E., Hildebrandt Ruiz, L., Hillamo, R., Jimenez, J. L., Junninen, H.,
679 Kiendler-Scharr, A., Kortelainen, A.-M., Kulmala, M., Laaksonen, A., Mensah, A.
680 A., Mohr, C., Nemitz, E., O'Dowd, C., Ovadnevaite, J., Pandis, S. N., Petäjä, T.,
681 Poulain, L., Saarikoski, S., Sellegri, K., Swietlicki, E., Tiitta, P., Worsnop, D. R.,
682 Baltensperger, U., and Prévôt, A. S. H.: Organic aerosol components derived from
683 25 AMS data sets across Europe using a consistent ME-2 based source
684 apportionment approach, Atmos. Chem. Phys., 14, 6159–6176,
685 doi:10.5194/acp-14-6159-2014, 2014.

686 Dimitroulopoulou, C., Ashmore, M. R., Byrne, M. A., and Kinnersley, R. P.:
687 Modelling of indoor exposure to nitrogen dioxide in the UK, Atmos. Environ., 35,
688 269–279, 2001.
689 Donahue, N. M., Tischuk, J. E., Marquis, B. J. and Huff Hartz, K. E.: Secondary
690 organic aerosol from limona ketone: insights into terpene ozonolysis via synthesis
691 of key intermediates, Phys. Chem. Chem. Phys., 9, 2991–2998, 2007.
692 Draper, D. C., Farmer, D. K., Desyaterik Y., and Fry, J. L.: A qualitative comparison
693 of secondary organic aerosol yields and composition from ozonolysis of
694 monoterpenes at varying concentrations of NO_2, Atmos. Chem. Phys., 15,
695 12267–12281, 2015.
696 Fry, J. L., Kiendler-Scharr, A., Rollins, A. W., Brauers, T., Brown, S. S., Dorn, H.-P.,
697 Dubé, W. P., Fuchs, H., Mensah, A., Rohrer, F., Tillmann, R.,Wahner,
698 A.,Wooldridge, P. J., and Cohen, R. C.: SOA from limonene: role of NO_3 in its
699 generation and degradation, Atmos. Chem. Phys., 11, 3879–3894,
700 doi:10.5194/acp-11-3879-3894., 2011.
701 Fry, J. L., Draper, D. C., Zarzana, K. J., Campuzano-Jost, P., Day, D. A., Jimenez, J.
702 L., Brown, S. S., Cohen, R. C., Kaser, L.,Hansel, A., Cappellin, L., Karl, T.,
703 Hodzic Roux, A., Turnipseed, A., Cantrell, C., Lefer, B., and Grossberg, N.:
704 Observations of gas- and aerosol-phase organic nitrates at BEACHON-RoMBAS
705 2011, Atmos. Chem. Phys., 13, 8585–8605, doi:10.5194/acp-13-8585-2013,
706 2013.
707 Gai, Y. B., Lin, X. X., Ma, Q., Hu, C. J., Gu, X. J., Zhao, W. X., Fang, B., Zhang, W.

J., Long, B., and Long, Z. W.: Experimental and theoretical study of reactions of OH radicals with hexenols: an evaluation of the relative importance of the H-abstraction reaction channel. Environ. Sci. Technol., 49, 10380–10388, 2015.

Geron, C., Rasmussen, R., Arnts, R. R., and Guenther, A.: A review and synthesis of monoterpene speciation from forests in the United States, Atmos. Environ., 34, 1761–1781,doi:10.1016/S1352-2310(99)00364-7, 2000.

Glausius, M., Lahaniati, M., Calogirou, A., DiBella, D., Jensen, N., Hjorth, J., Kotzias, D., and Larsen, B.: Carboxylic acids in secondary aerosols from oxidation of cyclic monoterpenes by ozone. Environ. Sci. Technol. 34, 1001–1010, 2000.

Griffin, R.J., Dabdub, D., and Seinfeld, J. H.: Secondary organic aerosol, 1. Atmospheric chemical mechanism for production of molecular constituents. J. Geophys. Res., [Atmos.], 107, 4332, DOI:10.1029/2001JD000541, 2002.

Griffin, R. J., Cocker III, D. R., Flagan, R. C., Seinfeld, J. H., and Dabdub, D.: Estimate of global atmospheric organic aerosol formation from the oxidation of biogenic hydrocarbons, Geophys. Res. Lett. 26, 2721–2724, 1999a.

Griffin, R. J., Cocker III, D. R., Flagan, R. C., and Seinfeld, J. H.: Organic aerosol formation from the oxidation of biogenic hydrocarbons, J. Geophys. Res., 104, 3555–3567, 1999b.

Guenther, A., Hewitt, C. N., Erickson, D., Fall, R., Geron, C., Graedel, T., Harley, P., Klinger, L., Lerdau, M., Mckay, W. A., Pierce, T., Scholes, B., Steinbrecher, R., Tallamraju, R., Taylor, J., and Zimmerman, P.: A global model of natural volatile organic compound emissions, J. Geophys. Res.-Atmos., 100, 8873–8892,

doi:10.1029/94JD02950, 1995.

Guenther, A., Geron, C., Pierce, T., Lamb, B., Harley, P., and Fall, R.: Natural emissions of non-methane volatile organic compounds, carbon monoxide, and oxides of nitrogen from North America. Atmos. Environ., 34, 2205–2230, 2000.

Hao, L. Q., Kortelainen, A., Romakkaniemi, S., Portin, H., Jaatinen, A., Leskinen, A., Komppula, M., Miettinen, P., Sueper, D., Pajunoja, A., Smith, J. N., Lehtinen, K. E. J.,Worsnop, D. R., Laaksonen, A., and Virtanen, A.: Atmospheric submicron aerosol composition and particulate organic nitrate formation in a boreal forestland–urban mixed region, Atmos. Chem. Phys., 14, 13483–13495, doi:10.5194/acp-14-13483-2014, 2014.

He, Y., Uno, I., Wang, Z., Ohara, T., Sugimoto, N., Shimizu, A., Richter, A., and Burrows J. P.: Variations of the increasing trend of tropospheric NO_2 over central east China during the past decade. Atmos. Environ., 41, 4865–4876, 2007.

Hoffmann, T., Odum, J. R., Bowman, F., Collins, D., Klockow, D., Flagan, R. C., and Seinfeld, J. H.: Formation of organic aerosols from the oxidation of biogenic hydrocarbons, J. Atmos. Chem., 26, 189–222, 1997.

Huang, M.Q., Hao, L.Q., Guo, X.Y., Hu, C. J., Gu, X. J., Zhao, W. X., Wang, Z.Y., Fang, L., and Zhang, W. J.: Characterization of secondary organic aerosol particles using aerosol laser time-of-flight mass spectrometer coupled with FCM clustering algorithm. Atmos. Environ., 64, 85–94, 2013.

Hynes, R. G., Angove, D. E., Saunders, S. M., Haverd, V., and Azzi, M.: Evaluation of two MCM v3.1 alkene mechanisms using indoor environmental chamber data,

752 Atmos. Environ., 39(38), 7251–7262, 2005.

753 Iinuma, Y., Böge, O., Gnauk, T., and Herrmann, H.: Aerosol chamber study of the
754 α-pinene/O_3 reaction: Influence of particle acidity on aerosol yields and products,
755 Atmos. Environ., 38, 761–773, 2004.

756 Jenkin, M. E., Saunders, S. M., and Pilling, M. J.: The tropospheric degradation of
757 volatile organic compounds: a protocol for mechanism development, Atmos.
758 Environ., 31, 81–104, 1997.

759 Jenkin, M. E.; Saunders, S. M.; Wagner, V.; Pilling, M. J. Protocol for the
760 development of the Master Chemical Mechanism, MCMv3 (Part B): tropospheric
761 degradation of aromatic volatile organic compounds, Atmos. Chem. Phys., 3,
762 181–193, 2003.

763 Jenkin, M. E., Young, J. C., and Rickard, A. R.: The MCM v3. 3.1 degradation
764 scheme for isoprene. Atmos. Chem. Phys., 15, 11433–11459, 2015.

765 Johnson, D., Jenkin, M. E.,Wirtz, K., and Martin-Reviejo, M.: Simulating the
766 formation of SOA from the photooxidation of aromatic hydrocarbons, Environ.
767 Chem., 2, 35–48, 2005.

768 Jonsson, Å. M., Hallquist, M., and Ljungström, E.: Impact of humidity on the ozone
769 initiated oxidation of limonene, Δ^3-carene, and α-pinene, Environ. Sci. Technol., 40,
770 188–194, 2006.

771 Jonsson, Å.M., Hallquist, M., and Ljungstrom, E.: Influence of OH scavenger on the
772 water effect on secondary organic aerosol formation from ozonolysis of limonene,
773 Δ^3-carene, and α-pinene, Environ. Sci. Technol., 42, 5938–5944, 2008a.

774 Jonsson, Å. M., Hallquist, M., and Ljungstro¨m, E.: The effect of temperature and
775 water on secondary organic aerosol formation from ozonolysis of limonene,
776 Δ^3-carene and α-pinene, Atmos. Chem. Phys., 8, 6541–6549, 2008b,
777 http://www.atmos-chem-phys.net/8/6541/2008/.
778 Kanakidou, M., Seinfeld, J. H., Pandis, S. N., Barnes, I., Dentener, F. J., Facchini, M.
779 C., Van Dingenen, R., Ervens, B., Nenes, A., Nielsen, C. J., Swietlicki, E., Putaud,
780 J. P., Balkanski, Y., Fuzzi,S., Horth, J., Moortgat, G. K., Winterhalter, R., Myhre,
781 C. E. L., Tsigaridis, K., Vignati, E., Stephanou, E. G., and Wilson, J.: Organic
782 aerosol and global climate modelling: a review, Atmos.Chem. Phys., 5, 1053–1123,
783 2005, http://www.atmos-chem-phys.net/5/1053/2005/.
784 Kiendler-Scharr, A., Mensah, A. A., Friese, E., Topping, D., Nemitz, E., Prevot, A. S.
785 H., Äijälä, M., Allan, J., Canonaco, F., Canagaratna, M., Carbone, S., Crippa, M.,
786 Dall Osto, M., Day, D. A., De Carlo, P., Di Marco, C. F., Elbern, H., Eriksson, A.,
787 Freney, E., Hao, L., Herrmann, H., Hildebrandt, L., Hillamo, R., Jimenez, J. L.,
788 Laaksonen, A., McFiggans, G., Mohr, C., O'Dowd, C., Otjes, R., Ovadnevaite, J.,
789 Pandis, S. N., Poulain, L., Schlag, P., Sellegri, K., Swietlicki, E., Tiitta, P.,
790 Vermeulen, A., Wahner, A., Worsnop, D., and Wu, H. C.: Organic nitrates from
791 night-time chemistry are ubiquitous in the European submicron aerosol, Geophys.
792 Res. Lett., 43, 7735–7744, doi:10.1002/2016GL069239, 2016.
793 Koch, S., Winterhalter, R., Uherek, E., Kolloff, A., Neeb, P., and Moortgat, G.:
794 Formation of new particles in the gas-phase ozonolysis of monoterpenes. Atmos.
795 Environ. 34, 4031–4042, 2000.

796 Kroll, J. H. and Seinfeld, J. H.: Chemistry of secondary organic aerosol: Formation
797 and evolution of low-volatility organics in the atmosphere, Atmos. Environ., 42,
798 3593–3624, 2008.
799 Kroll, J. H., Ng, N. L., Murphy, S. M., Flagan, R. C., and Seinfeld, J. H.: Secondary
800 organic aerosol formation from isoprene photooxidation, Environ. Sci. Technol., 40,
801 1869–1877, 2006.
802 Kulmala, M., Asmi, A., Lappalainen, H. K., Baltensperger, U., Brenguier, J.-L.,
803 Facchini, M. C., Hansson, H.-C., Hov, Ø., O'Dowd, C. D., Pöschl, U.,
804 Wiedensohler, A., Boers, R., Boucher, O., de Leeuw, G., Denier van der Gon, H. A.
805 C., Feichter, J., Krejci, R., Laj, P., Lihavainen, H., Lohmann, U., Mc-Figgans, G.,
806 Mentel, T., Pilinis, C., Riipinen, I., Schulz, M., Stohl, A., Swietlicki, E., Vignati, E.,
807 Alves, C., Amann, M., Ammann, M., Arabas, S., Artaxo, P., Baars, H., Beddows, D.
808 C. S., Bergström, R., Beukes, J. P., Bilde, M., Burkhart, J. F., Canonaco, F., Clegg,
809 S. L., Coe, H., Crumeyrolle, S., D'Anna, B., Decesari, S., Gilardoni, S., Fischer, M.,
810 Fjaeraa, A. M., Fountoukis, C., George, C., Gomes, L., Halloran, P., Hamburger, T.,
811 Harrison, R. M., Herrmann, H., Hoffmann, T., Hoose, C., Hu, M., Hyvärinen, A.,
812 Hõrrak, U., Iinuma, Y., Iversen, T., Josipovic, M., Kanakidou, M., Kiendler-Scharr,
813 A., Kirkevåg, A., Kiss, G., Klimont, Z., Kolmonen, P., Komppula, M., Kristjánsson,
814 J.-E., Laakso, L., Laaksonen, A., Labonnote, L., Lanz, V. A., Lehtinen, K. E. J.,
815 Rizzo, L. V., Makkonen, R., Manninen, H. E., McMeeking, G., Merikanto, J.,
816 Minikin, A., Mirme, S., Morgan, W. T., Nemitz, E., O'Donnell, D., Panwar, T. S.,
817 Pawlowska, H., Petzold, A., Pienaar, J. J., Pio, C., Plass-Duelmer, C., Prévôt, A. S.

818 H., Pryor, S., Reddington, C. L., Roberts, G., Rosenfeld, D., Schwarz, J., Seland, Ø.,
819 Sellegri, K., Shen, X. J., Shiraiwa, M., Siebert, H., Sierau, B., Simpson, D., Sun, J.
820 Y., Topping, D., Tunved, P., Vaattovaara, P., Vakkari, V., Veefkind, J. P.,
821 Visschedijk, A., Vuollekoski, H., Vuolo, R., Wehner, B., Wildt, J., Woodward, S.,
822 Worsnop, D. R., van Zadelhoff, G.-J., Zardini, A. A., Zhang, K., van Zyl, P. G.,
823 Kerminen, V.-M., S Carslaw, K., and Pandis, S. N.: General overview: European
824 Integrated project on Aerosol Cloud Climate and Air Quality interactions
825 (EUCAARI) – integrating aerosol research from nano to global scales, Atmos.
826 Chem. Phys., 11, 13061–13143, doi:10.5194/acp-11-13061-2011, 2011.
827 Leungsakul, S., Jaoui, M., and Kamens, R.M.: Kinetic mechanism for predicting
828 secondary organic aerosol formation from the reaction of d-limonene with ozone.
829 Environ. Sci. Technol., 39, 9583–9594, 2005.
830 Madronich, S. and Calvert, J. G.: Permutation reactions of organic peroxy radicals in
831 the troposphere, J. Geophys. Res., 95(D5), 5697–5715, 1990.
832 Maksymiuk, C. S., Gayahtri, C., Gil, R. R., and Donahue, N. M.: Secondary organic
833 aerosol formation from multiphase oxidation of limonene by ozone: mechanistic
834 constraints via two-dimensional heteronuclear NMR spectroscopy. Phys. Chem.
835 Chem. Phys., 11, 7810–7818, 2009.
836 Mylonas, D. T., Allen, D. T., Ehrman, S. H., and Pratsinis, S. E.: The sources and size
837 distributions of organonitrates in Los Angeles aerosol. Atmos. Environ., 25,
838 2855–2861, 1991.
839 Nah, T., McVay, R. C., Zhang, X., Boyd, C. M., Seinfeld, J. H., and Ng, N. L.:

Influence of seed aerosol surface area and oxidation rate on vapor wall deposition and SOA mass yields: a case study with α-pinene ozonolysis. Atmos. Chem. Phys., 16, 9361–9379, 2016

Nazaroff, W.W. and Weschler, C.J.: Cleaning products and air fresheners: exposure to primary and secondary air pollutants. Atmos. Environ., 38, 2841–2865, 2004.

Ng, N. L., Kroll, J. H., Keywood, M. D., Bahreini, R., Varutbangkul, V., Flagan, R. C., and Seinfeld, J. H.: Contribution of first- versus second-generation products to secondary organic aerosols formed in the oxidation of biogenic hydrocarbons. Environ. Sci. Technol., 40, 2283-2297, 2006.

Ng, N. L., Kroll, J. H., Chan, A. W. H., Chhabra, P. S., Flagan, R. C., and Seinfeld, J. H.: Secondary organic aerosol formation from m-xylene, toluene, and benzene, Atmos. Chem. Phys., 7, 3909–3922, 2007a, http://www.atmos-chem-phys.net/7/3909/2007/.

Ng, N. L., Chhabra, P. S., Chan, A. W. H., Surratt, J. D., Kroll, J. H., Kwan, A. J., McCabe, D. C., Wennberg, P. O., Sorooshian, A., Murphy, S. M., Dalleska, N. F., Flagan, R. C., and Seinfeld, J. H.: Effect of NO_x level on secondary organic aerosol (SOA) formation from the photooxidation of terpenes, Atmos. Chem. Phys., 7, 5159–5174, 2007b, http://www.atmos-chem-phys.net/7/5159/2007/.

Ng, N. L., Brown, S.S., Archibald, A.T., Atlas, E., Cohen, R.C., Crowley, J. N., Day, D. A., Donahue, N. M., Fry, J. L., Fuchs, H., Griffin, R. J., Guzman, M. I., Herrmann, H., Hodzic, A., Iinuma,Y., Jimenez, J. L., Kiendler-Scharr, A., Lee, B. H., Luecken, D. J., Mao, J., McLaren, R., Mutzel, A., Osthoff, H. D., Ouyang, B.,

862 Picquet-Varrault, B., Platt, U., Pye, H. O. T., Rudich,Y., Schwantes, R. H., Shiraiwa,
863 M., Stutz, J., Thornton, J. A., Tilgner, A., Williams, B. J., and Zaveri, R. A.: Nitrate
864 radicals and biogenic volatile organic compounds: oxidation, mechanisms, and
865 organic aerosol, Atmos. Chem. Phys., 17, 2103–2162, 2017
866 Nojgaard, J. K., Bilde, M., Stenby, C., Nielsen, O. J., and Wolkoff, P.: The effect of
867 nitrogen dioxide on particle formation during ozonolysis of two abundant
868 monoterpenes indoors. Atmos. Environ., 40, 1030–1042, 2006.
869 Odum, J. R., Hoffmann, T., Bowman, F., Collins, D., Flagan, R. C., and Seinfeld, J.
870 H.: Gas/particle partitioning and secondary organic aerosol yields, Environ. Sci.
871 Technol., 30, 2580–2585,1996.
872 Pan, G., Hu, C. J., Wang, Z.Y., Cheng, Y., Zheng, X. H., Gu, X. J., Zhao, W. X.,
873 Zhang, W. J., Chen, J., Liu, F. Y., Shan, X. B., and Sheng, L. S.: Direct detection
874 of isoprene photooxidation products by using synchrotron radiation
875 photoionization mass spectrometry. Rapid Commun. Mass Spectrom., 26,
876 189–194, 2012.
877 Pan, X., Underwood, J. S., Xing, J. H., Mang, S. A., and Nizkorodov, S. A.:
878 Photodegradation of secondary organic aerosol generated from limonene
879 oxidation by ozone studied with chemical ionization mass spectrometry, Atmos.
880 Chem. Phys., 9, 3851–3865, 2009.
881 Palen, E. J., Allen, D. T., Pandis, S. N., Paulson, S. E., Seinfeld, J. H., and Flagan, R.
882 C.: Fourier transform infrared analysis of aerosol formed in the photo-oxidation of
883 isoprene and beta-pinene, Atmos. Environ., 26, 1239–1251, 1992.

884 Pankow, J. F.: An absorption model of the gas/aerosol partitioning of organic
885 compounds in the atmosphere, Atmos.Environ., 28(6), 185–188, 1994a.
886 Pankow, J. F.: An absorption model of the gas/aerosol partitioning involved in the
887 formation of secondary organic aerosol, Atmos.Environ., 28(6), 189–193, 1994b.
888 Pathak, R. K., Salo, K., Emanuelsson, E. U., Cai, C., Lutz, A., Hallquist, Å. M., and
889 Hallquist, M. Influence of ozone and radical chemistry on limonene organic
890 aerosol production and thermal characteristics. Environ. Sci. Technol., 46,
891 11660−11669, 2012.
892 Pinho, P. G., Pio, C. A., and Jenkin, M. E.: Evaluation of isoprene degradation in the
893 detailed tropospheric chemical mechanism, MCM v3, using environmental
894 chamber data, Atmos. Environ., 39, 1303–1322, 2005.
895 Pinho, P. G., Pio, C. A., Carter, W. P. L., and Jenkin, M. E.: Evaluation of α- and
896 β-pinene degradation in the detailed tropospheric chemistry mechanism, MCM
897 v3.1, using environmental chamber data, J. Atmos. Chem., 57(2), 171–202, 2007.
898 Presto, A. A., Hartz, K. E. H., and Donahue, N. M.: Secondary organic aerosol
899 production from terpene ozonolysis. 1. Effect of UV radiation, Environ. Sci.
900 Technol., 39, 7036–7045, 2005a.
901 Presto, A. A., Hartz, K. E. H., and Donahue, N. M.: Secondary organic aerosol
902 production from terpene ozonolysis. 2. Effect of NO_x concentration, Environ. Sci.
903 Technol., 39, 7046–7054, 2005b.
904 Rollins, A. W., Browne, E. C., Min, K. E., Pusede, S. E., Wooldridge, P. J., Gentner,
905 D. R., Goldstein, A. H., Liu, S., Day, D. A., Russell, L. M., and Cohen, R. C.:

Evidence for NOx Control over Nighttime SOA Formation, Science, 337, 1210–1212, 2012.

Saathoff, H., Naumann, K.-H., Möhler, O., Jonsson, Å. M., Hallquist, M., Kiendler-Scharr, A., Mentel, Th. F., Tillmann, R., and Schurath, U.: Temperature dependence of yields of secondary organic aerosols from the ozonolysis of α-pinene and limonene, Atmos. Chem. Phys., 9, 1551–1577, 2009, http://www.atmos-chem-phys.net/9/1551/2009/.

Sarwar, G., Corsi, R., Allen, D., Weschler, C.: The significance of secondary organic aerosol formation and growth in buildings: experimental and computational evidence. Atmos. Environ., 37, 1365−1381, 2003.

Saunders, S. M., Jenkin, M. E., Derwent, R. G., and Pilling, M. J.: Protocol for the development of the Master Chemical Mechanism, MCM v3 (Part A): tropospheric degradation of nonaromatic volatile organic compounds, Atmos. Chem. Phys., 3, 161–180, doi:10.5194/acp-3-161-2003, 2003.

Seinfeld, J. H., and Pandis, S. N.: Atmospheric Chemistry and Physics: From Air Pollution to Climate Change, vol. 27, 1326 pp., John Wiley, New York, 1998.

Seinfeld, J. H. and Pankow, J. F.: Organic atmospheric particulate material, Annu. Rev. Phys. Chem., 54, 121–140, 2003.

Setyan, A., Zhang, Q., Merkel, M., Knighton, W. B., Sun, Y., Song, C., Shilling, J. E., Onasch, T. B., Herndon, S. C.,Worsnop, D. R., Fast, J. D., Zaveri, R. A., Berg, L. K., Wiedensohler, A., Flowers, B. A., Dubey, M. K., and Subramanian, R.: Characterization of submicron particles influenced by mixed biogenic and

928 anthropogenic emissions using high-resolution aerosol mass spectrometry: results
929 from CARES, Atmos. Chem. Phys., 12, 8131–8156,
930 doi:10.5194/acp-12-8131-2012, 2012.
931 Shu, Y. and Atkinson, R.: Rate constants for the gas-phase reactions of O_3 with a
932 series of terpenes and OH radical formation from the O_3 reactions with
933 sesquiterpenes at 296 ±2 K. Int. J. Chem. Kinet., 26, 1193−1205, 1994.
934 Singer, B. C., Destaillats, H., Hodgson, A. T., and Nazaroff, W. W.: Cleaning
935 products and air fresheners: emissions and resulting concentrations of glycol
936 ethers and terpenoids. Indoor Air, 16, 179–191, 2006.
937 Socrates, G.: Infrared and Raman Characteristic Group Frequencies: Tables and
938 Charts, 3rd ed., John Wiley and Sons, Ltd.: New York, 2001.
939 Song, C., Na, K. S., and Cocker, D. R.: Impact of the hydrocarbon to NO_x ratio on
940 secondary organic aerosol formation, Environ. Sci. Technol., 39, 3143–3149, 2005.
941 Song, C., Na, K. S., Warren, B., Malloy, Q., and Cocker, D. R.: Secondary organic
942 aerosol formation from m-xylene in the absence of NO_x. Environ. Sci. Technol.,
943 41, 7409–7419, 2007.
944 Spittler, M., Barnes, I., Bejan, I., Brockmann, K. J., Benter, T., and Wirtz, K.:
945 Reactions of NO_3 radicals with limonene and alphapinene: Product and SOA
946 formation, Atmos. Environ., 40, S116–S127, 2006.
947 Stroud, C., Makar, P., Karl, T., Guenther, A., Geron, C., Turnipseed, A., Nemitz, E.,
948 Baker, B., Potosnak, M., and Fuentes, J. D.: Role of canopy-scale photochemistry
949 in modifying biogenic-atmosphere exchange of reactive terpene species: Results

from the CELTIC field study, J. Geophys. Res., 110, D17303, 2005.

Topping, D., Barley, M., Bane, M. K., Higham, N., Aumont, B., Dingle, N. McFiggans, G.: UManSysProp v1.0: an online and open-source facility for molecular property prediction and atmospheric aerosol calculations, Geosci. Model Dev., 9(2), 899–914, 2016.

Wainman, T., Zhang, J., Weschler, C. J., and Lioy, P. J.: Ozone and limonene in indoor air: a source of submicron particle exposure. Environ. Health Perspect., 108(12), 1139–1145, 2000.

Walser, M. L., Desyaterik, Y., Laskin, J., Laskin, A., and Nizkorodov, S. A.: High-resolution mass spectrometric analysis of secondary organic aerosol produced by ozonation of limonene, Phys. Chem. Chem. Phys., 10, 1009–1022, 2008.

Waring, M. S.: Secondary organic aerosol in residences: predicting its fraction of fine particle mass and determinants of formation strength, Indoor Air, 24 (4), 376–389 , 2014

Weschler, C. J. and Shields, H. C. Indoor ozone/terpene reactions as a source of indoor particles. Atmos. Environ., 33, 2301–2312, 1999.

Weschler, C. J., Shields, H. C., and Nalk, D. V.: Indoor chemistry involving O_3, NO and NO_2 as evidenced by 14 months of measurements at a site in southern California. Environ. Sci. Technol., 28, 2120–2131, 1994.

WHO.: Indoor Air Quality Guidelines for Europe, second edition. WHO Regional Publications, European series., No 91, 175–179, 2000.

Wirtz, K., and Martin-Reviejo, M.: Density of secondary organic aerosols. J. Aerosol Sci., 34, S223–S224, 2003.

Xia, A. G., Michelangeli, D. V., and Makar, P. A.: Box model studies of the secondary organic aerosol formation under different HC/NO_x conditions using the subset of the Master Chemical Mechanism for α-pinene oxidation, J. Geophys. Res., [Atmos.],113(10), DOI: 10.1029/2007JD008726, 2008.

Xu, J., Griffin, R. J., Liu,Y., Nakao, S., and Cocker III, D. R.: Simulated impact of NO_x on SOA formation from oxidation of toluene and m-xylene, Atmos. Environ., 101, 217–225, 2015.

Xu, L., Guo, H., Boyd, C. M., Klein, M., Bougiatioti, A., Cerully, K. M., Hite, J. R., Isaacman-VanWertz, G., Kreisberg, N. M., Knote, C., Olson, K., Koss, A., Goldstein, A. H., Hering, S. V., de Gouw, J., Baumann, K., Lee, S.-H., Nenes, A., Weber, R. J., and Ng, N. L.: Effects of anthropogenic emissions on aerosol formation from isoprene and monoterpenes in the southeastern United States, P. Natl. Acad. Sci. USA, 112, 37–42, 2015a.

Xu, L., Suresh, S., Guo, H., Weber, R. J., and Ng, N. L.: Aerosol characterization over the southeastern United States using high resolution aerosol mass spectrometry: spatial and seasonal variation of aerosol composition and sources with a focus on organic nitrates, Atmos. Chem. Phys., 15, 7307–7336, doi:10.5194/acp-15-7307-2015, 2015b.

Yarwood, G., Rao, S., Yocke, M., and Whitten, G. Z.: Final Report - Updates to the Carbon Bond Chemical Mechanism: CB05. 2005.

994 Zhang, J. Y., Huff Hartz, K. E., Pandis S. N., and Donahue, N. M.: Secondary organic
995 aerosol formation from limonene ozonolysis: Homogeneous and heterogeneous
996 influences as a function of NO_x, J. Phys. Chem. A, 110, 11053–11063, 2006.

997
998
999
1000
1001
1002
1003
1004
1005
1006
1007
1008
1009
1010
1011
1012
1013
1014
1015

Figure Captions:

Figure 1. Observed (points) and predicted (lines) concentration profiles of limonene (purple squares), O_3 (blue filled triangles), NO_2 (red dots) and SOA (diamonds-raw; filled squares-corrected) versus reaction time for Exp. N19.

Figure 2. Aerosol yield for the limonene/O_3/NO_2 system for the initial terpene mixing ratios of ~ 125 ppb with NO_2 (~250 ppbv) or without NO_2. Each data point represents an individual experiment.

Figure 3. SOA growth as a function of initial NO_2 concentration under the constant $[O_3]_0/[VOC]_0$ ratio ($[O_3]_0/[VOC]_0$ ratio~2.5).

Figure 4. Comparison of the observed SOA yield and the predicted SOA yield for all the smog chamber experiments. The sizes of the data points represent the corresponding initial O_3 levels of the simulated experiments, and the color scale represents corresponding initial NO_2 levels. The line is linear fit to illustrate the relativity between the predicted SOA yield and the observed SOA yield. (Number 1-21 above the data points corresponds to Experiment N1-N21 shown in Table 1)

Figure 5. FTIR spectra of the particle products collected with PTFE filters from a high NO_2 experiment (upper panel), a low NO_2 experiment (medium panel), and a blank experiment (lower panel).

Figure 6. Changes of ROOHs, acids, PANs, and nitrates with different initial mixing ratio of the NO_2 (A) in gas phase, (B) in aerosol phase, and (C) in both phase.

Figure 7. Aerosol mass fraction of the 20 dominant condensable compounds at different initial concentration of NO_2.

Atmos. Chem. Phys. Discuss., https://doi.org/10.5194/acp-2017-433
Manuscript under review for journal Atmos. Chem. Phys.
Discussion started: 15 June 2017

Atmospheric Chemistry and Physics Discussions

Scheme 1. Major reaction paths in the initial ozonolysis and NO_3 oxidation of limonene.(Species in solid boxes are condensable compounds which can be partition to the organic aerosol phase. Species in solid boxes with shadow are those contribute dominantly to SOA in this simulation as listed in Table **S1**. Species in dashed box refer to the reactive radicals which generally will react further. Broken arrows indicate there are multi-step reaction not shown, which result in further degradation of the related species.)

Atmos. Chem. Phys. Discuss., https://doi.org/10.5194/acp-2017-433
Manuscript under review for journal Atmos. Chem. Phys.
Discussion started: 15 June 2017

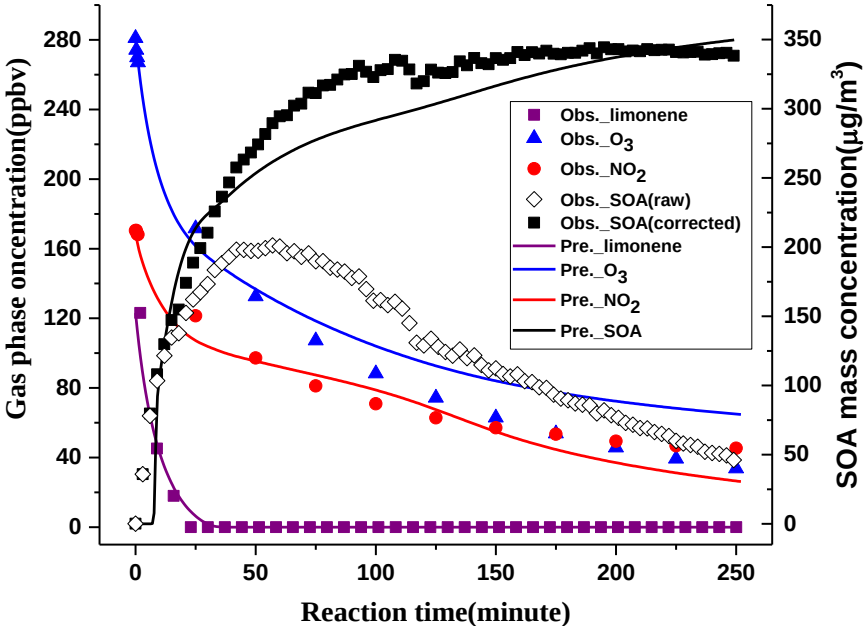

Figure 1. Hu *et al*

Atmos. Chem. Phys. Discuss., https://doi.org/10.5194/acp-2017-433
Manuscript under review for journal Atmos. Chem. Phys.
Discussion started: 15 June 2017

Atmospheric Chemistry and Physics Discussions

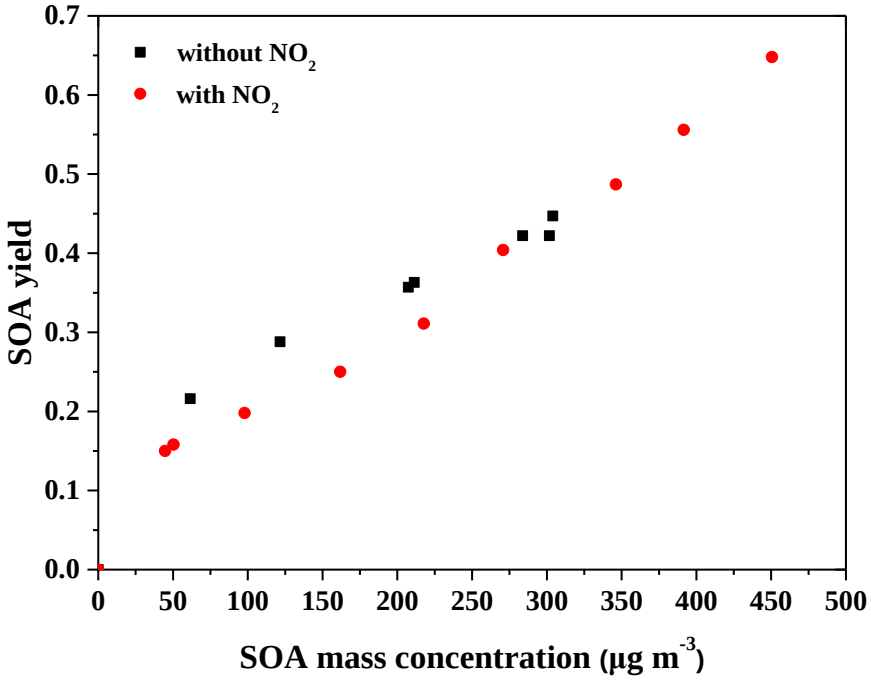

Figure 2. Hu *et al*

Atmos. Chem. Phys. Discuss., https://doi.org/10.5194/acp-2017-433
Manuscript under review for journal Atmos. Chem. Phys.
Discussion started: 15 June 2017

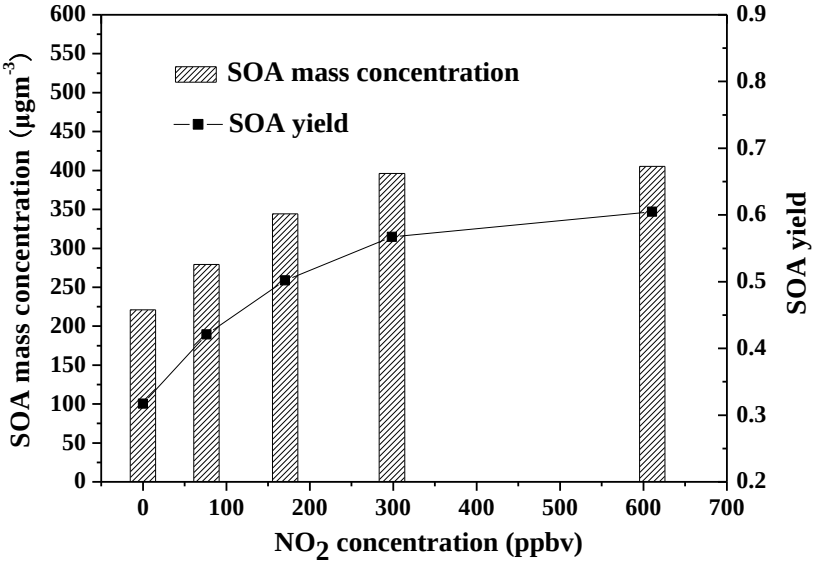

Figure 3. Hu *et al*

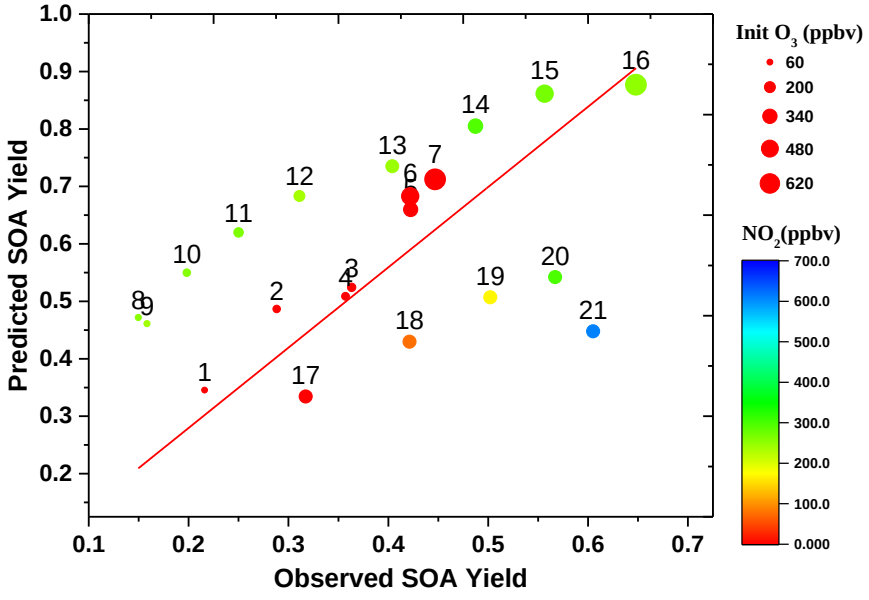

Figure 4. Hu *et al*

Atmos. Chem. Phys. Discuss., https://doi.org/10.5194/acp-2017-433
Manuscript under review for journal Atmos. Chem. Phys.
Discussion started: 15 June 2017

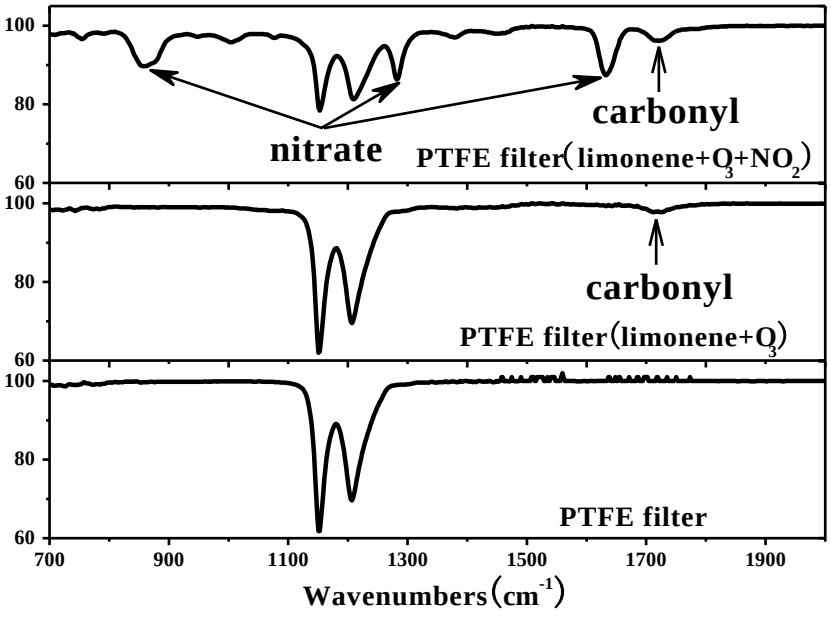

Figure 5. Hu *et al*

Atmos. Chem. Phys. Discuss., https://doi.org/10.5194/acp-2017-433
Manuscript under review for journal Atmos. Chem. Phys.
Discussion started: 15 June 2017

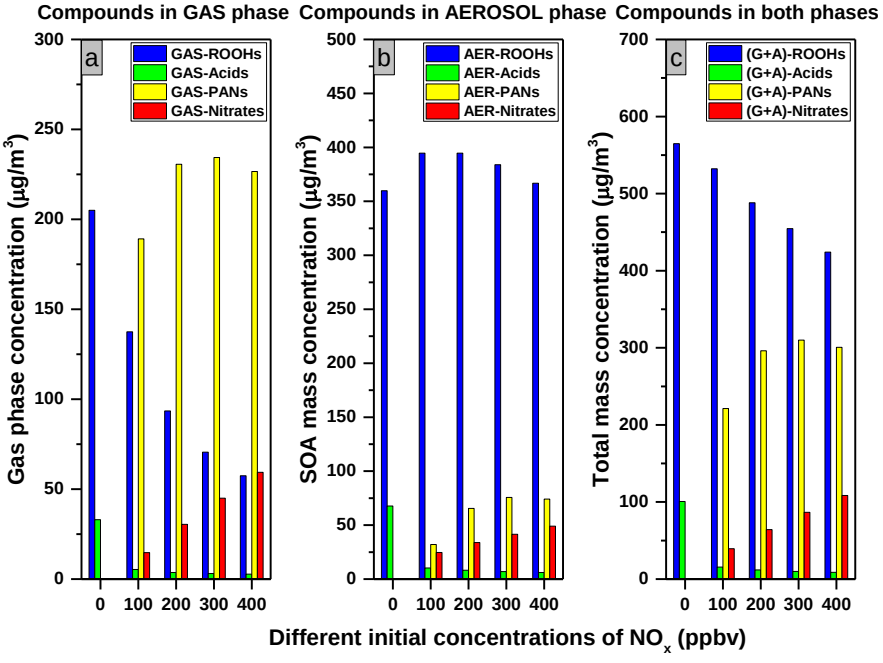

Figure 6. Hu *et al*

Atmos. Chem. Phys. Discuss., https://doi.org/10.5194/acp-2017-433
Manuscript under review for journal Atmos. Chem. Phys.
Discussion started: 15 June 2017

Atmospheric Chemistry and Physics Discussions

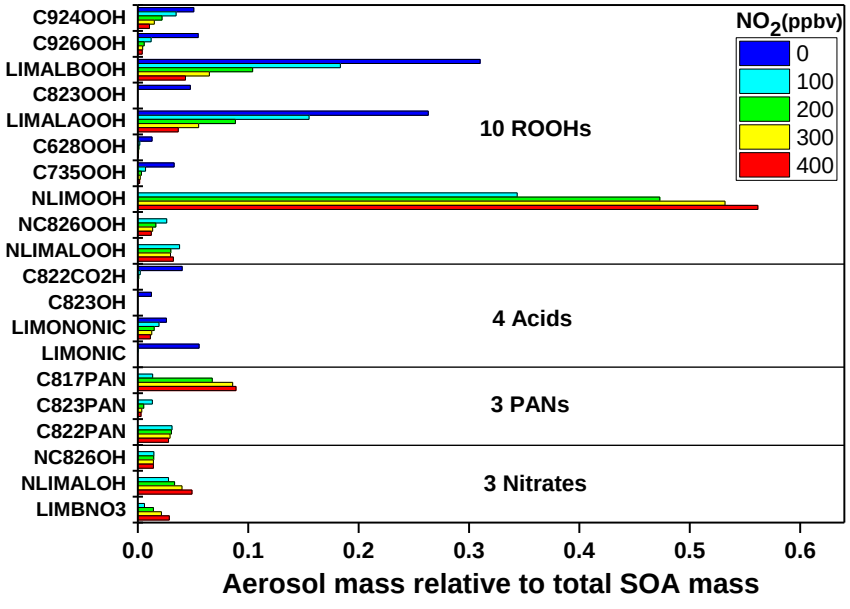

Figure 7. Hu *et al*

Atmos. Chem. Phys. Discuss., https://doi.org/10.5194/acp-2017-433
Manuscript under review for journal Atmos. Chem. Phys.
Discussion started: 15 June 2017

Atmospheric Chemistry and Physics Discussions

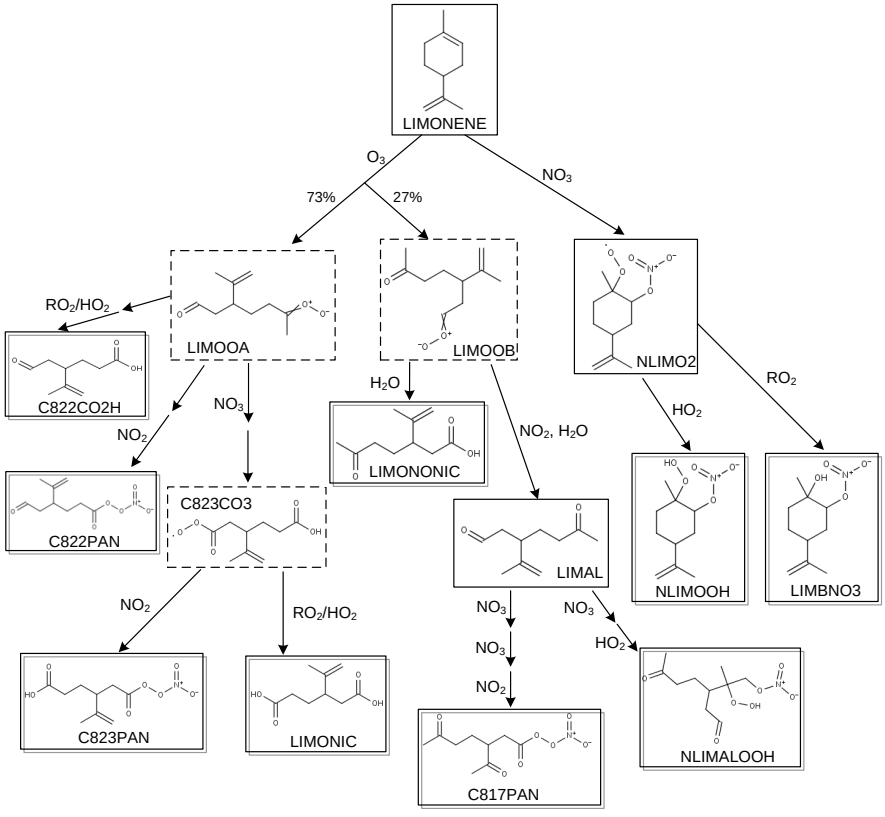

Scheme 1. Hu *et al*

Atmos. Chem. Phys. Discuss., https://doi.org/10.5194/acp-2017-433
Manuscript under review for journal Atmos. Chem. Phys.
Discussion started: 15 June 2017

Atmospheric Chemistry and Physics Discussions

Table 1 Summary of experimental conditions and results in the presence or absence of NO_2 [a]

Expt. No.	HC_0 (ppbv)	$[O_3]_0$ (ppbv)	ΔHC (ppbv)	ΔHC ($\mu g/m^3$)	$[NO_2]_0$ (ppbv)	M_0 ($\mu g/m^3$)	SOA Yield
N 1	130	~60	51.1	285	<1 [c]	61.5	0.216
N 2	127	~100	75.7	422	<1 [c]	122	0.288
N 3	123	~120	104	582	<1 [c]	211	0.363
N 4	126	~110	104	581	<1 [c]	207	0.357
N 5	128	~350	128	714	~2 [c]	302	0.422
N 6	121	~500	121	673	~3 [c]	284	0.422
N 7	122	~700	122	680	~3 [c]	304	0.447
N 8	124	~70	53.6	299	256	44.7	0.150
N 9	128	~70	57.1	318	240	50.4	0.158
N 10	128	~100	88.6	494	259	97.9	0.198
N 11	126	~160	116	647	264	162	0.250
N 12	126	~210	126	700	237	218	0.311
N 13	120	~250	120	670	245	271	0.404
N 14	128	~360	128	710	293	346	0.487
N 15	126	~500	126	704	270	392	0.556
N 16	125	~700	125	695	251	451	0.648
N 17 [b]	125	~300	125	697	<2 [c]	221	0.317
N 18 [b]	119	~300	119	663	76.2	279	0.421
N 19 [b]	123	~300	123	686	170	344	0.502
N 20 [b]	125	~300	125	699	299	396	0.567
N 21 [b]	120	~300	120	700	611	405	0.605

[a] Experiments were carried out at temperature of 18.4±1.6℃, and relative humidity of 12.8%±2.5%. [b] Experiments were carried out at temperature of 25.4±0.8 ℃, and relative humidity of 14.5%±0.7%. [c] the minor NO_2 was produce from corona-discharge when O_3 was produced.

Atmos. Chem. Phys. Discuss., https://doi.org/10.5194/acp-2017-433
Manuscript under review for journal Atmos. Chem. Phys.
Discussion started: 15 June 2017

Atmospheric Chemistry and Physics Discussions

Table 2. The names, structures and formulas of the top 20 condensable compounds according to their organic aerosol mass fraction.

Name	Structure	Formula	Name	Structure	Formula
C924OOH	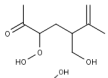	$C_9H_{16}O_4$	C822CO2H	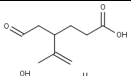	$C_9H_{14}O_3$
C926OOH	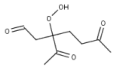	$C_9H_{14}O_5$	C823OH	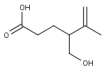	$C_8H_{14}O_3$
LIMALBOOH	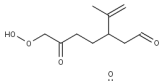	$C_{10}H_{16}O_4$	LIMONONIC	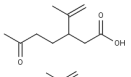	$C_{10}H_{16}O_3$
C823OOH	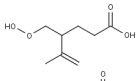	$C_8H_{14}O_4$	LIMONIC	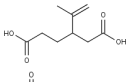	$C_9H_{14}O_4$
LIMALAOOH	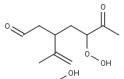	$C_{10}H_{16}O_4$	C817PAN	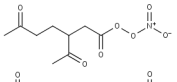	$C_9H_{13}NO_7$
C628OOH		$C_6H_{10}O_5$	C823PAN	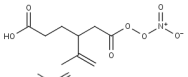	$C_9H_{13}NO_7$
C735OOH	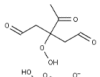	$C_7H_{10}O_5$	C822PAN	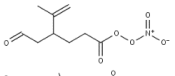	$C_9H_{13}NO_6$
NLIMOOH		$C_{10}H_{17}NO_5$	NC826OH	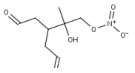	$C_8H_{13}NO_6$
NC826OOH	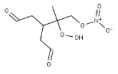	$C_8H_{13}NO_7$	NLIMALOH	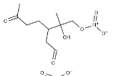	$C_{10}H_{17}NO_6$
NLIMALOOH	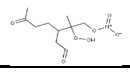	$C_{10}H_{17}NO_7$	LIMBNO3		$C_{10}H_{17}NO_4$